Simulation Study on Harmonic Torque Injection for Suppressing Flow Pulsations in Electrified Axial Piston Pumps

Thomas Heeger and Liselott Ericson

Dep. of Management and Engineering, Fluid and Mechatronic Systems,
Linköping University, 581 83 Linköping, Sweden
E-mail: thomas.heeger@liu.se; liselott.ericsson@liu.se

Abstract

Noise is one of the major challenges for the electrification of hydraulic systems for mobile working machinery. Without the masking sounds of a combustion engine, the distinct noise of the hydraulic pump becomes more audible and thus needs to be reduced. Compressible pump flow pulsations caused by imperfect commutation are one of the main noise sources.

Electric motor control offers the possibility to inject torque pulses at the pump's first harmonic frequency in order to reduce common noise. This paper uses lumped parameter simulation to drive a hydraulic pump with different shapes of drive torques, and in different operating conditions. The potential of injecting harmonics into the drive torque for the reduction of flow pulsations is explored. At the right phase and amplitudes, these pulses can basically eliminate flow pulsations at their frequency. Scaling laws for comparisons of different piston numbers are summarised, and the behaviour of a 9 and a 10 piston pump are compared, demonstrating that lower torque amplitudes are required when using smaller piston numbers. Required torque amplitudes are quantified, showing that torque amplitudes in the region multiples of the pump's ideal drive torque are required at medium or high speeds. Furthermore, these torque amplitudes significantly increase losses and increase the requirements for the inverter, making harmonic injection impractical at medium and high speeds. At low speeds, the first pump harmonic can be eliminated, but this is of limited benefit due to the low sensitivity of human hearing at these frequencies.

Keywords: axial piston pump, electric motor, flow pulsations, fluid power, harmonic injection, noise

1 Introduction

Conventional mobile fluid power systems such as excavators and wheel loaders often exhibit low efficiency, with estimations of around 21% in 2012 [1] or around 30% in 2017 [2]. Due to concern about greenhouse gas emissions and the rising energy cost, different approaches to increase energy efficiency are investigated, e.g., using energy recovery and avoiding throttling losses [3]. One mayor trend is electrification, leading to the combination of electric motors with hydraulic pumps [4].

Whilst a lot of research focuses on efficiency, noise is also of large relevance for health, customer acceptance, and legislation [5]. Due to the disappearance of the masking noise of the combustion engine, the noise of the hydraulic pump becomes more audible. The interaction between hydraulic pump and electric motor for noise generation is however not very well researched. A previous paper of the authors showed that the combination of pole numbers and pistons affects the common noise [6]. This highlights the need to consider both electric motor and hydraulic pump for noise emission, and to design them for optimisation of their combined noise.

2 Literature Review

There are several contributors to noise, both in hydraulic and electric machines. For details on the hydraulic noise contributors, refer to the books by Ivantysyin and Ivantysynova [7], and Manring [8] on hydraulic pumps. Amongst others, Heeger et al. [9] described various commutation features used to reduce hydraulic pump noise. However, none of the methods fully eliminates force/moment and flow ripples. It is still not fully understood which ripple is the main contributor to noise, and it can depend on the system installation. However, typically, the pump flow ripple is believed to be a main contributor for hydraulic system noise and thus a main focus. Furthermore, Ericson et al. [10] showed that minimising the flow ripple reduces the other noise contributors as well.

Minav et al. [11] investigated using variable electric motor speed in order to eliminate / reduce an axial piston pump's flow ripple. They considered the kinematic flow ripple, but neglected the compressible flow ripple. Reference speeds to counteract the kinematic flow ripple with an opposing speed ripple were computed. They concluded that the torque capability of the electric motor limits the compensation capability. The required accelerations (and therefore torque) increase with higher speeds, so flow ripple compensation is especially challenging at higher speeds.

O'Shea [12] aimed to overcome this limitation using a low inertia gerotor pump and a feed-forward control algorithm, and the study was limited to reducing the first harmonic. At an average speed of around 400 rpm, significant reductions of the pressure ripple were measured using this strategy. However, similar to Minav et al. [11], limitations for higher frequencies were stated.

Mikota and Manhartsgruber [13] suggested passive control of the pump pulsations using a dedicated compensator, which is located between the prime mover and the hydraulic machine. Simulation showed that a coupling using a lightly damped torsional oscillator can create an antiresonance. If the antiresonance matches the first pump harmonic, pulsations at that harmonic can be reduced. A challenge is that the antiresonance frequency depends on the entire pump drivetrain dynamics, including some parameters such as damping which possess some uncertainty.

Liang et al. [14] developed a controller for a switched reluctance machine to drive a hydraulic pump. They aimed to reduce the torque ripple of the switched reluctance machine, and to avoid pressure overshoots when changing operating points.

Mehta [15] and Manring et al. [16] claimed that torque ripple might be the main cause of noise, referring to unpublished measurements. Mehta [15] further showed a correlation of torque and flow pulsations, under the assumption of incompressible fluids and simplified pressure profiles. For a reduction of torque ripple, swash plate oscillations were suggested. Furthermore, it was shown that tandem pump design significantly reduces the kinematic torque ripple if the offset angle is half a period for even piston numbers or quarter of a period for odd piston numbers.

Heeger et al. [6] summarised the harmonic noise contributors in electrically driven pumps and investigated different pistons numbers in combination with a 12 slot 10 pole PMSM. This work also showed combinations of e-motor torque and pump torque, and opened the question on whether an optimisation for a co-design for reduced torque pulsations is possible.

This paper aims to investigate the relevance of the type of torque ripple an electric machine transmits to a hydraulic pump on the other noise contributors in the system.

In comparison to the works of Minav et al. [11] and O'Shea [12], this contributes detailed pump simulations which consider compressible effects. The behaviour for different piston numbers is investigated based on the example of a 9 and a 10 piston pump, as odd and even piston numbers have different inherent properties. Scaling laws for rotation group geometry, pressure relief groove geometry and inertia are applied to provide a fair comparison between different piston numbers. Furthermore, this work considers the damping properties of a hydraulic volume at the pump outlet. Additionally, torque data from PMSM simulations is fed to the simulation model to demonstrate the feasibility of harmonic cancellation when combining it with a torque ripple at the pump's harmonic frequency. Lastly, different aspects such as electromagnetic losses due to harmonic injection, human hearing sensitivity at low frequencies and the angular position of the pump relative to the electric motor are discussed.

3 Simulation Model

This section gives an overview on the structure and assumptions of the simulation model and the used torque inputs. Furthermore, the scaling of inputs for comparable results for different numbers of pistons z are summarised.

3.1 Pump Model

This study uses a lumped parameter model in Hopsan [17] and is structured as shown in Figure 1. The model is capable of simulating different types of axial piston machines, and this study is done on the example of a machine of floating piston type [18].

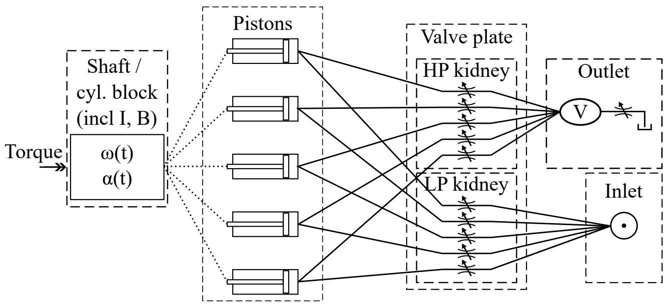

Figure 1: Schematic of Hopsan model structure.

The shaft / cylinder block component includes the torque balance as shown in Equation 1. The lever L_i of each piston's force f_i around the drive axis is computed based on the shaft angle α and the pump's geometry.

$$T = \sum_{i=1}^{n} F_i L_i + I\dot{\omega} + B\omega \tag{1}$$

Each piston's velocity v_i is computed using equation 2.

$$v_i = \omega L_i \tag{2}$$

For each piston, the force balance (Equation 3) and the continuity equation (Equation 4) are solved. The effective bulk modulus β_e is computed under the consideration of the piston's chamber pressure and pseudo cavitation.

$$F = Ap \tag{3}$$

$$\sum q = \frac{dV_{cyl}}{dt} + \frac{V_{cyl}}{\beta_e}\frac{dp}{dt} \tag{4}$$

The inlet and outlet ports are modelled as orifices with variable areas, which are computed based on the rotational angle α. The inlet port is connected to a constant pressure source. The outlet is modelled as a volume, followed by an orifice and tank. The simulation model neglects leakage.

3.2 Estimation of the Friction Coefficient

To estimate the friction coefficient B, a simple surrogate model as shown in Equation 5 is used. The parameters a, b and c are fitted to test data. B summarises the friction of all components.

$$T_{\mathrm{loss}} = a \cdot p + b \cdot n + c \tag{5}$$

Figure 2 shows a comparison of the surrogate model to the measurement data it was fitted to. The R^2 value is 0.916, which is acceptable considering the simplicity of the model and that e.g., mixed lubrication at low speeds is not captured by it.

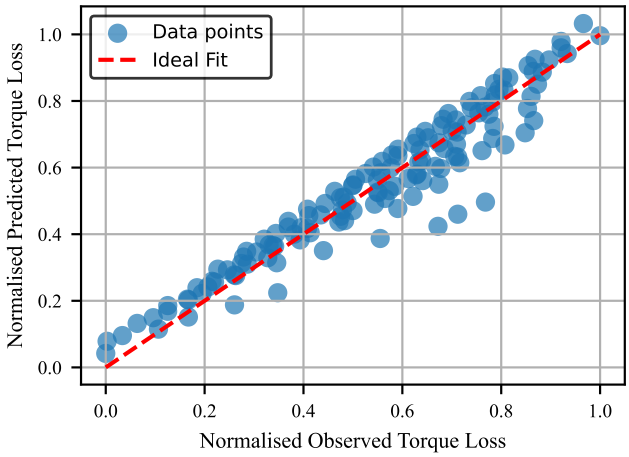

Figure 2: Normalised measured torque loss in comparison to surrogate model.

For the sake of simplicity, this work uses the same coefficients for Equation 5 independent of the number of pistons of the pump.

3.3 Scaling of Rotating Group Geometry

As the combination of piston number and pole pair number is expected to affect noise, pumps with different numbers of pistons are to be simulated. To ensure a fair comparison, the rotating group geometry is designed using the scaling laws presented by Achten [19]. Therefore, the displacement (35 cc/rev), displacement angle (8 deg) and piston pitch ratio (0.22) are kept constant, and the piston area and cylinder block pitch diameter are scaled.

3.4 Scaling of Inertia

The inertia of a cylinder follows Equation 6.

$$J_{\mathrm{cyl}} = \frac{1}{2} m r^2 \tag{6}$$

Assuming that the piston pitch radius R_{pp} is representative for r, and that the mass of the rotating parts scales with R_{pp}^3, yields Equation 7.

$$J_{\mathrm{pump}} \propto R_{\mathrm{pp}}^5 \tag{7}$$

The piston pitch radius R_{pp} can be taken from the scaling of the geometry of the rotating group (see Equation 8), with k being 1 for a regular pump and 2 for a tandem pump.

$$R_{\mathrm{pp}} \propto \frac{1}{z^{\frac{1}{3}} \left(\sin\left(\frac{\pi k}{zk}\right)\right)^{\frac{2}{3}}} \tag{8}$$

Finally, the inertia of pump J_{pump} and the inertia of the electric motor J_{EM} are added in Equation 9. The inertia of the electric motor is independent of the number of pistons. In this study, the electric motor's inertia is roughly 15 times larger than the pump's inertia and therefore dominates Equation 9.

$$J_{\mathrm{tot}} = J_{\mathrm{pump}} + J_{\mathrm{EM}} \tag{9}$$

3.5 Scaling of Pressure Relief Grooves

Pressure relief groove design plays a crucial role for pump noise. Palmberg [20] derived Equations 10 and 11 for the length and final area of pressure relief grooves.

$$l_{\mathrm{g}} = R\sqrt{\frac{2\alpha_{\mathrm{p}} h\, p_0}{\beta}} \tag{10}$$

$$A_{\mathrm{g}} = \frac{(1+n)D\omega}{C_{\mathrm{q}} z}\sqrt{\frac{\alpha_{\mathrm{p}}\rho}{h\beta}} \tag{11}$$

The bulk modulus β, the density ρ, the orifice coefficient C_{q}, the displacement D, the shaft frequency ω, the exponent in the orifice area function n, and the system pressure p_0 are not (or negligibly) affected by a change of the number of pistons. Assuming a constant dead volume ratio, the clearance volume factor α_{p} also remains constant.

The flow gradient h scales according to Equation 12.

$$h \propto \frac{1}{z} \tag{12}$$

Assuming that the piston pitch radius R_{pp} and the pressure relief groove pitch radius R are identical results in the scaling laws for the groove's length l_{g} and final area A_{g} as shown in Equations 13 and 14.

$$l_{\mathrm{g}} \propto R_{\mathrm{pp}}\sqrt{\frac{1}{z}} \propto \frac{1}{z^{\frac{5}{6}} \left(\sin\left(\frac{\pi k}{zk}\right)\right)^{\frac{2}{3}}} \tag{13}$$

$$A_{\mathrm{g}} \propto \frac{1}{z^{3/2}} \tag{14}$$

4 Results for Sine Shaped Torque Pulsations

For the torque input, the following set-ups were used:

- Constant torque input.
- Constant torque input combined with a sine shaped pulsation as shown in Equation 15.
- Look-up table based torque input, using results from Ansys Motorcad simulations for a 12 slot 10 pole permanent magnet synchronous machine. This is done in Section 5.

$$T = T_{\text{ave}} + T_{\text{amplitude}} \cdot \sin\left(z \cdot \alpha + \phi\right) \tag{15}$$

This section shows results for constant torque inputs as well as for sine shaped torque pulsations following Equation 15. Effects of varying different simulation parameters on speed, flow and pressure pulsations are investigated. Also, pumps with 9 and 10 pistons were considered as the noise emission of pumps with odd and even piston numbers differs significantly.

4.1 Effect of Phase of Torque Pulsation

Previous work by the authors [6] suggested using the combination of the electric motor's and hydraulic pump's torque ripples to reduce the combined ripple. Typically, the first harmonic dominates the flow pulsations' frequency spectrum of axial piston pumps. Therefore, a sine shaped torque pulsation is added to a constant drive torque to investigate the potential for noise reduction. Harmonic injection is used in electric motor control to reduce the motor's torque ripple [21], but in principle the motor control could also be used to artificially create a torque ripple. Different phase shifts can either amplify or reduce the ripples.

4.1.1 Definition of Phase Shift

The significance of the phase of the torque pulsation is investigated by testing the baseline case (without torque pulsation), and applying a torque pulsation of 5 Nm amplitude at first fundamental piston frequency. This is done for 20 different phase shifts, differing by 5% of a period. A rotation angle of 0 degrees is defined when the first piston is at the center of its suction stroke as visualised in Figure 3. That means that the commutation to connect to the high-pressure kidney starts after 25% (or 90°) of a period for the 9 piston pump, and after 50% (or 180°) of a period for the 10 piston pump.

4.1.2 Effect on Speed and Flow Pulsations

The phase of the torque pulsation changes the phase of the speed pulsations as well as the amplitude at the first piston frequency, see Figures 4 and 5.

The speed ripple alters the flow ripple significantly.

For the 9 piston pump, Figure 6 shows that flow pulsations are reduced when the torque pulsation is 15% of a period ahead. This results in the peak of the speed ripple (see Figure 4) coinciding with the valley of the flow ripple. For a 10 Nm torque ripple, the first fundamental is reduced by 79% in comparison to the baseline. The higher harmonics are not significantly affected, which is reasonable considering that the input torque signal did not contain their frequencies.

Figure 7 shows a similar situation for the 10 piston pump. For a phase shift of 95%, the first fundamental is reduced by 42%.

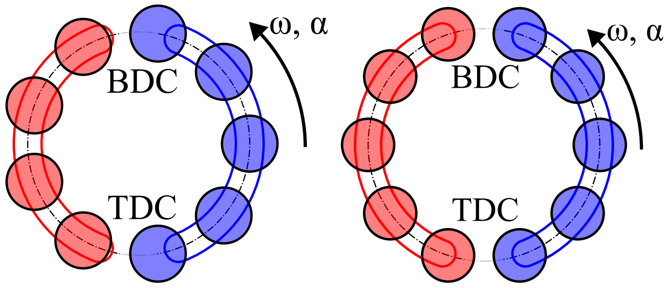

(a) α=0 for 9 piston pump. *(b) α=0 for 10 piston pump.*

Figure 3: Definition of 0 degree position.

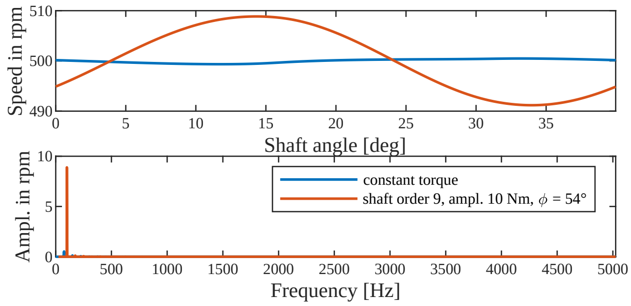

Figure 4: Speed pulsations for constant torque and a 10 Nm amplitude torque ripple with 15% period phase shift for a 9 piston pump operated at 500 rpm and 50 bar.

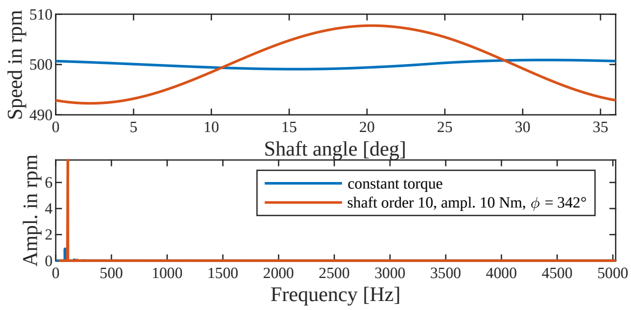

Figure 5: Speed pulsations for constant torque and a 10 Nm amplitude torque ripple with 95% period phase shift for a 10 piston pump, operating at 500 rpm and 50 bar.

4.1.3 Methodology for Finding Optimal Phase Shift

For a given pump and operating condition, the optimal phase shift is found by simply comparing the first harmonic of the flow ripple for different phase shifts. Exemplary results can be seen in Figure 8.

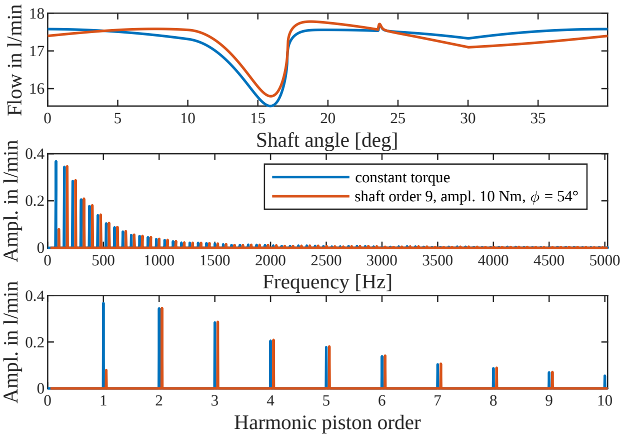

Figure 6: Flow pulsations for constant torque and a 10 Nm amplitude torque ripple with 15% phase shift for a 9 piston pump, operating at 500 rpm and 500 bar.

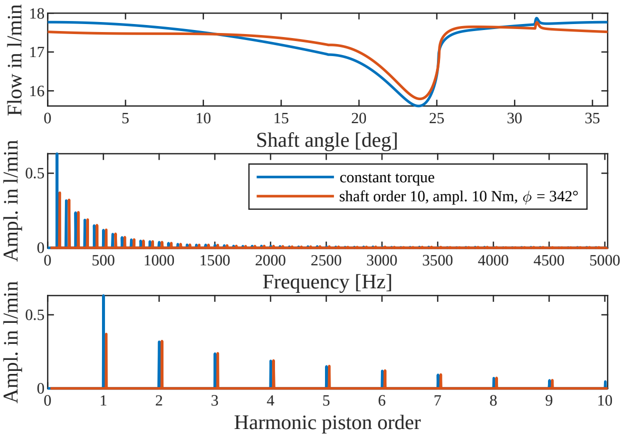

Figure 7: Flow pulsations for constant torque and a 10 Nm amplitude torque ripple with 95% phase shift for a 10 piston pump, operating at 500 rpm and 50 bar.

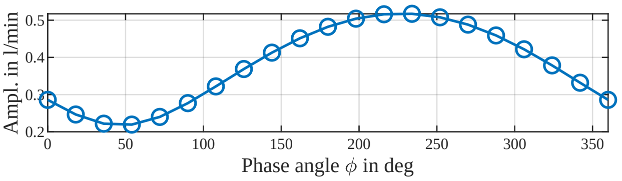

Figure 8: Phase shift dependency of first fundamental harmonic on the phase shift. The example is for a 9 piston pump, 50 bar, 500 rpm, and 5 Nm amplitude.

4.1.4 Effect of Operating Conditions

The previous results showed operation at 50 bar and 500 rpm. However, it is also of interest how the ideal phase changes with changing operating conditions. At this stage, the torque amplitude is fixed to 50 Nm. A parameter sweep over 20 phase shifts is used to identify the ideal phase shift for each operating point. Tables 1 and 2 show that the operating point has some effect on the ideal phase angle, as the commutation is affected both by the pressure and speed level.

Table 1: Ideal Phase Shift for 9 Piston Pump in Percent of a Period (in increments of 5), for a torque amplitude of 50 Nm.

	50 bar	200 bar	350 bar
500 rpm	15	10	10
2000 rpm	10	5	5
4000 rpm	10	0	0

Table 2: Ideal Phase Shift for 10 Piston Pump in Percent of a Period (in increments of 5), for a torque amplitude of 50 Nm.

	50 bar	200 bar	350 bar
500 rpm	95	90	85
2000 rpm	90	85	80
4000 rpm	90	80	75

4.2 Effect of Amplitude of Torque Pulsation

The torque amplitude controls the amplitude of the speed pulsation. A too small amplitude has no significant effect, and a too high amplitude overcompensates for the pump's inherent flow pulsations.

Previously, arbitrary torque amplitudes were used to find good phase shifts. In this chapter, torque amplitudes are optimised for fixed phase shifts.

At 500 rpm and 50 bar, a torque amplitude of 12 Nm with a phase shift of 13% is applied to the 9 piston machine. Figure 9 shows that the first fundamental is almost completely eliminated with a reduction of 99.8%.

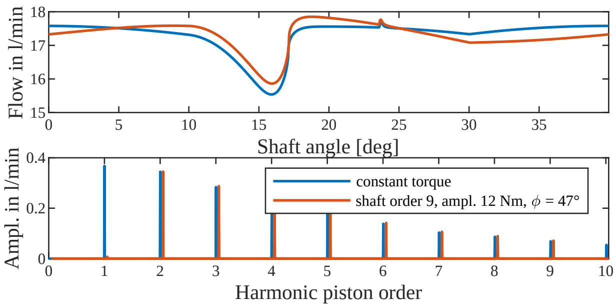

Figure 9: Flow pulsations for 9 piston machine with optimised torque amplitude at 500 rpm and 50 bar.

The 10 piston machine behaves similarly. A torque amplitude of 24 Nm is applied at a phase shift of 93% to the 10 piston machine. As shown in Figure 10, this yields an almost complete elimination of the first fundamental with a reduction of 97%.

A complete elimination of the first harmonic is feasible with a finer tuning of the phase angle and amplitude of the torque pulsation.

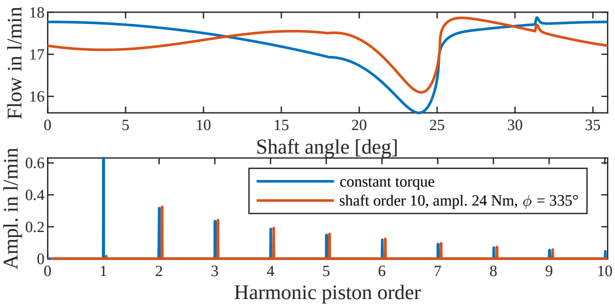

Figure 10: Flow pulsations for 10 piston machine with optimised torque amplitude at 500 rpm and 50 bar.

4.2.1 Effect of Operating Conditions

Tables 3 and 5 show the ideal torque amplitudes to eliminate the first fundamental under consideration of the pump's and the electric motor's inertia. As a comparison, Tables 4 and 6 show the torque amplitudes required when only considering the pump's inertia, i.e., neglecting the electric motor's inertia. A comparison of the tables shows that the electric motor's inertia increases the required torque amplitudes by one order of magnitude. Note that the phase angles in Tables 1 and 2 were used for all tables.

Table 3: Ideal Torque Amplitude for 9 Piston Pump in Nm (considering inertia of pump and electric machine).

	50 bar	200 bar	350 bar
500 rpm	12	28	43
2000 rpm	200	430	650
4000 rpm	820	1670	2540

Table 4: Ideal Torque Amplitude for 9 Piston Pump in Nm when only considering pump inertia (neglecting the inertia of the electric machine).

	50 bar	200 bar	350 bar
500 rpm	1.0	2.0	3.5
2000 rpm	15	32	49
4000 rpm	61	124	189

Table 5: Ideal Torque Amplitude for 10 Piston Pump in Nm (considering inertia of pump and electric machine).

	50 bar	200 bar	350 bar
500 rpm	24	39	52
2000 rpm	370	550	750
4000 rpm	1430	1970	2700

Note that in line with Minav et al. [11] and O'Shea [12], for higher speeds, higher torque amplitude are required for more significant reductions, and the practical limitations due

Table 6: Ideal Torque Amplitude for 10 Piston Pump in Nm when only considering pump inertia (neglecting the inertia of the electric machine).

	50 bar	200 bar	350 bar
500 rpm	2.0	3.0	4.5
2000 rpm	31	46	61
4000 rpm	125	169	228

to the high required amplitudes are confirmed. In addition, the torque amplitude increases with increasing pressures.

The 10 piston machine requires higher torque amplitudes for all operating points. This is caused by a higher frequency requiring faster accelerations as well as higher inertia. The effect is more profound at low and medium pressures than at high pressures.

4.2.2 Importance of First Harmonic

Pressure relief grooves are most effective in reducing harmonics of second and higher order. However, the first harmonic typically is only slightly reduced [22], and remains as the major noise contributor. Therefore, a torque pulsation capable of eliminating the first harmonic is a significant contribution to noise reduction.

4.3 Effect of Frequency of Torque Pulsation

Up to this point, torque pulsations of the first fundamental were considered. However, the first fundamental of the inherent torque pulsation of a 12 slot 10 pole permanent magnet synchronous machine is at 30 times the shaft frequency [6]. This chapter investigates the behaviour of the pumps in combination with a torque pulsation according to Equation 16.

$$T = T_{\mathrm{ave}} + T_{\mathrm{amplitude}} \cdot \sin(30 \cdot \alpha + \phi) \tag{16}$$

In case of the 9 piston pump, this does not coincide with any pump harmonics. Therefore, as visualised in Figure 11, adding the torque pulsations simply leads to additional frequency content of the flow pulsation, independent of the phase of the torque pulsations.

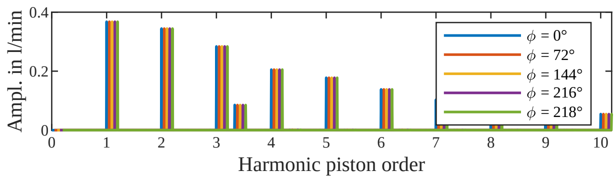

Figure 11: Harmonics at 50 bar and 500 rpm for the 9 piston machine and a torque pulsation of 30 times shaft frequency for different phase angles.

In case of the 10 piston pump, this coincides with the third harmonic. Therefore, as Figure 12 visualises, depending on the phase angle, the third pump harmonic is either reinforced or weakened. Table 7 shows the ideal phase shift for different operating conditions. As the ideal phase shift differs between operating conditions, there is not one single ideal positioning of the electric motor to the hydraulic pump.

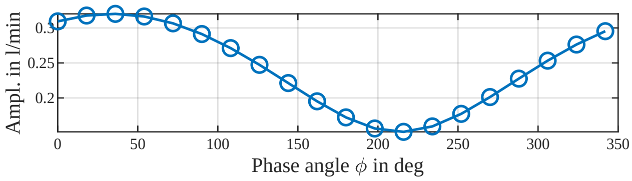

Figure 12: Phase angle dependency of third harmonic of 10 piston machine for a torque pulsation running at 30 times shaft frequency. Example is done for 50 bar, 500 rpm, and 10 Nm amplitude.

Table 7: Ideal Phase Shift for 10 Piston Pump to Reduce the Third Harmonic (in Percent of a Period and in increments of 5)

	50 bar	200 bar	350 bar
500 rpm	60	55	50
2000 rpm	35	25	20
4000 rpm	30	15	0

4.4 Effect of Volume

Up to this point, a volume of 100 ml at the pump outlet was considered.

However, the size of the volume affects the damping, and therefore the flow pulsations are reduced by the volume. This section investigates the influence of the volume size by comparing the system behaviour for a volume of 10 ml, 100 ml, and 1000 ml.

A parameter sweep showed that the ideal phase shift and torque amplitude are not significantly affected by the volume at the pump outlet. Figure 13 shows the flow pulsations before the volume for the same operating conditions and different volumes. Figure 14 shows the flow pulsations for the same operating condition after the volume. The smallest volume (10 ml) has very little damping, but the larger volumes (100 ml, 1000 ml) show significantly reduced flow pulsations after the volume.

Figure 15 shows the ratio of the harmonics before and after the volume, confirming that higher order harmonics decrease more than low-order harmonics.

5 Results for Torque Pulsations of a PMSM

In this section, the interaction of the torque pulsations of a 12 slot 10 pole permanent magnet synchronous machine with the pump setups are investigated. For this purpose, a lookup table with the rotational angle and the instantaneous torque is created using Ansys Motorcad and fed to the Hopsan pump model.

Figure 16 shows the inherent torque curves of the PMSM and

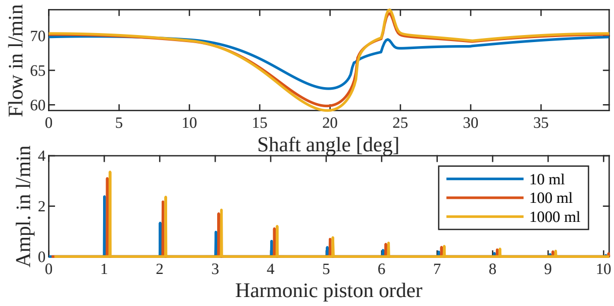

Figure 13: Flow before the volume at 200 bar and 2000 rpm for the 9 piston machine with constant torque for different volumes.

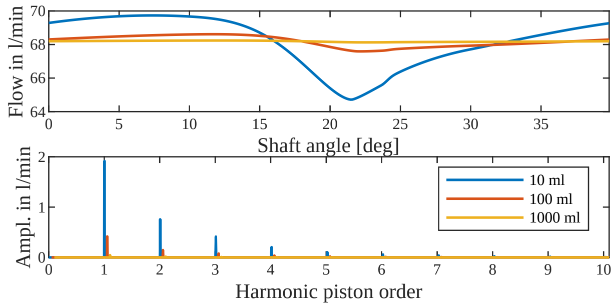

Figure 14: Flow after the volume at 200 bar and 2000 rpm for the 9 piston machine with constant torque for different volumes.

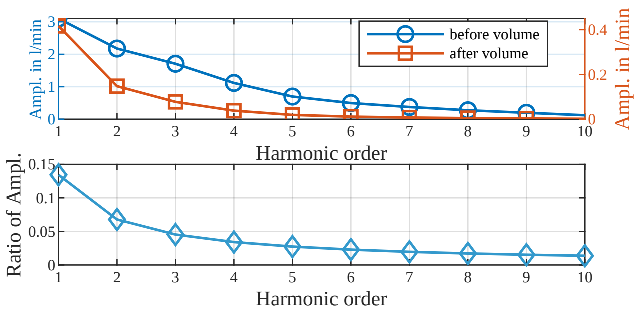

Figure 15: Increased damping of higher harmonics based on 9 piston pump operating at 2000 rpm and 200 bar and 100 ml volume.

the pumps. The average PMSM torque is larger than for the pumps due to friction.

Figure 17 shows the flow pulsations after a 100 ml volume for a constant torque source in comparison to the PMSM with different relative positions to the pump. The PMSM acts very similar to the constant torque source.

Figure 18 shows the flow for different relative positions of the PMSM to a 10 piston pump whose first harmonic is suppressed by a first order torque pulsation. The torque suppression works for either orientation, and only negligible differences for the third harmonic are observed.

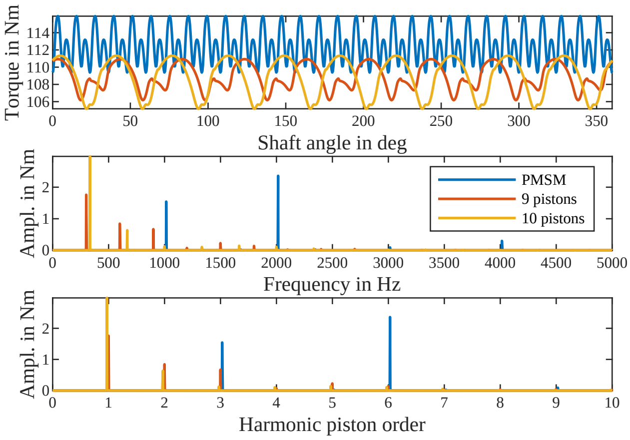

Figure 16: Inherent torque curves 12 slot 10 pole PMSM and 9 resp. 10 piston pump for operation at 200 bar and 2000 rpm. Note that for the PMSM, the 10 piston machine was used to define the harmonic piston orders.

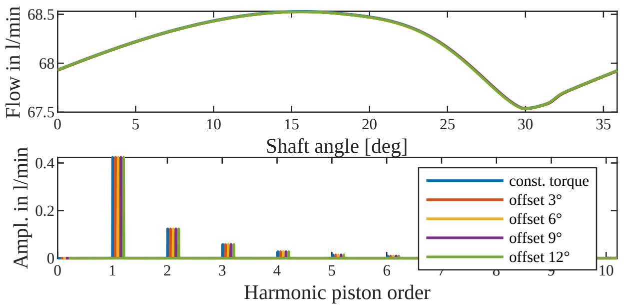

Figure 17: Flow after a 100 ml volume for a 10 piston pump driven by a constant torque or a 12 slot 10 pole PMSM with different positional offsets. The example is for operation at 200 bar and 2000 rpm.

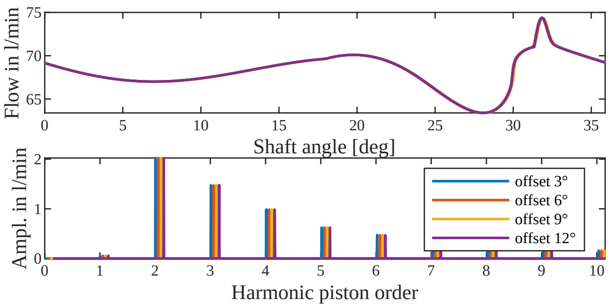

Figure 18: Flow pulsations for different positions of the PMSM relative to a 10 piston pump with eliminated first harmonic for operation at 2000 rpm and 200 bar.

6 Discussion

This section discusses the implications of the results on the choice of number of pistons, the feasibility and usefulness to create the required torque ripples, electromagnetic losses, and refinements to the presented method.

6.1 Effect of the Number of Pistons

In principle, the reduction of the first harmonic works the same independent of the piston number. However, comparing Tables 3 and 5 shows that the 10 piston pump requires higher torque amplitudes than the 9 piston pump. This is caused both by the decreased time a period requiring faster accelerations and by an increased inertia.

Using 10 pistons in combination with a 12 slot 10 pole PMSM offers the possibility to use the electric machine's inherent torque ripple to reduce the pump's third harmonic. However, Table 7 shows that the ideal phase has some spread, and Figure 18 showed that the effect of the angular orientation of the PMSM on the third pump harmonic is negligible.

6.2 Torque Requirement

It is in principle possible to use torque/speed pulsations to eliminate harmonics of the flow pulsations, but medium or high speeds require very high torque amplitudes (as already stated by Minav et al. [11] and O'Shea [12]). In comparison to Minav et al.'s work, the torque amplitudes are significantly higher due to increased inertia, and the consideration of compressible flow. The electric motor's inertia is one order of magnitude higher than the pump's inertia, and is therefore the main driver of the torque requirements. A low number of pistons leads to higher inherent pump pulsations, but they are easier to cancel using a torque pulse as they provide increased acceleration time and decreased inertia.

The considered displacement (35 cc/rev) in combination with the considered maximum pressure (350 bar) yields an ideal drive torque of 195 Nm. Tables 3 and 5 show that for low speeds, only small torque amplitudes are needed. At medium and high speeds, torque amplitudes of some 100 Nm or higher are required. This is expected to exceed the feasible torque ripple for the electric motor and a standard inverter.

6.3 Human Hearing

The human hearing area spans frequencies from 20 Hz to 20 kHz. However, the sensitivity of human hearing is frequency-dependent and e.g. sounds of with los frequencies need higher sound pressure levels to be perceived than sounds at medium frequencies [23].

When operating a 9-piston pump at 500 rpm, the first fundamental frequency is 75 Hz. As the human ear is not very sensitive at these frequency, removing the first harmonic from an audio signal has no audible effect.

6.4 Losses

Losses in PMSM are typically dominated by copper losses and iron losses. Harmonic injection increases the losses of the electric motor [21], which reduces the efficiency and creates additional heat in the electric motor. Note that even the inverter losses increase with increasing switching frequencies, but this will not be quantified in this paper.

6.4.1 Copper Losses

Copper losses follow Ohm's law, see Equation 17.

$$P_{\mathrm{loss,Cu}} = R_{\mathrm{el}} I_{\mathrm{rms}}^2 \tag{17}$$

For surface-mounted PMSM outside the field-weakening region, the current is approximately proportional to the torque. Therefore, copper losses scale approximately with the square of the torque.

Equation 18 describes the current as a function of time, yielding Equation 19 giving an expression of the square of the rms current I_{rms}^2, which is proportional to the copper losses $P_{loss,Cu}$. Equation 19 enables an estimation of the increase of the copper losses due to harmonic injection. The exemplary results in Tables 8 and 9 show a slight increase of copper losses due to harmonic injection at low speeds, but very high increases at medium speeds.

$$I(t) = I_{\mathrm{ave}} + I_{\mathrm{amp}} \cdot \sin(k\omega t) \tag{18}$$

$$I_{\mathrm{rms}}^2 = I_{\mathrm{ave}}^2 + \frac{I_{\mathrm{amp}}^2}{2} \tag{19}$$

Table 8: Increase of copper losses caused by harmonic injection of amplitudes as given in Table 3 for a 9 piston machine.

	50 bar	200 bar	350 bar
500 rpm	9.3%	3.2%	2.4%
2000 rpm	2578%	745%	556%

Table 9: Increase of copper losses caused by harmonic injection of amplitudes as given in Table 5 for a 10 piston machine.

	50 bar	200 bar	350 bar
500 rpm	37.1%	6.1%	3.6%
2000 rpm	8824%	1219%	740%

6.4.2 Iron Losses

Iron losses consist of the hysteresis losses, eddy losses and excess losses which cannot be explained by the two aforementioned loss mechanisms, and are generally estimated according to Equation 20 [24].

$$P_{\mathrm{loss,Fe}} = k_{\mathrm{h}} f B_{\mathrm{stator}}^{\alpha_{\mathrm{h}}} + k_{\mathrm{cl}} f^2 B_{\mathrm{stator}}^2 + k_{\mathrm{exc}} f^{1.5} B_{\mathrm{stator}}^{1.5} \tag{20}$$

The equation shows a sensitivity both to frequency and magnitude of flux variations. Sohail Ahmed [25] made measurements with different harmonics at different frequencies. For a fundamental frequency of 50 Hz, introducing a harmonic with an amplitude of 20% of the base value yielded a maximum loss increase of 85% for a 7th order harmonic and 168% for an 11th order harmonic. For the 9 piston machine at 500 rpm, the ratio is in a similar region, so iron losses in a similar order of magnitude are to be expected. For the 10 piston machine, the torque ratio is higher, thus higher increases of iron losses are to be expected.

6.5 Positioning of PMSM relative to the Pump

For the considered example, Figure 18 implies that the positioning of the PMSM relative to the pump is only of minor importance, as it only affects the third pump harmonic in this case, and the magnitude changes are very small. Furthermore, Table 7 shows that an ideal position for all operating points cannot be found anyway.

For other electric motor configurations, these conclusions may however not be valid as they possess other frequencies and amplitudes.

6.6 Improvements to the Method

The parameter sweeps done in Sections 4.1 and 4.2 show the potential of drastic reductions of the first fundamental harmonic. A co-optimisation of phase angle and torque amplitude could however yield even better results.

7 Conclusion

This paper investigated the idea to intentionally introduce speed pulsations with the electric motor to cancel the first harmonic of the hydraulic pump's flow pulsation in order to reduce common noise.

Due to the large inertia of the electric motor, the angular orientation between the pump and the electric motor does not significantly affect the pump's flow pulsations.

Pressure relief grooves are a typical commutation feature to reduce flow pulsations from hydraulic pumps. However, they only have a small effect on the first order harmonics, which often dominate a pump's frequency spectrum. Motor control can be used to induce torque pulsations at the pump's first harmonic, and using the correct amplitude and phase, the pump's first harmonic can be eliminated. Unfortunately, due to the electric motor's large inertia, very large torque amplitudes in the order of multiples of nominal torque are required to cancel the first harmonic at medium and high speeds. Also, higher piston numbers require larger amplitudes, as higher frequencies require higher accelerations, and as inertia typically increased with higher piston numbers. These large torque amplitudes cause unreasonable levels of currents. Furthermore, electromagnetic losses drastically increase due to the required amplitudes at medium and high speeds. At low speeds, the torque amplitudes are in a reasonable region, and losses are slightly increased. Therefore, the cancellation of the first harmonic is in principle feasible. However, at these speeds, the first harmonic is at frequencies where the human ear is not very sensitive, yielding almost no audible benefit of removing this harmonic.

Therefore, introducing speed pulsations to the electric motor is no practical method of eliminating the first harmonic of hydraulic flow pulsations.

Acknowledgement

This research was funded by the Swedish Electromobility Centre with grant number 13070 and the Swedish Energy Agency (Energimyndigheten) with grant number P2023-00594.

Nomenclature

Designation	Denotation	Unit
α	Shaft angle	rad
α_{h}	Hysteresis loss exponent	-
α_{p}	Clearance volume factor	-
β_{e}, β	(Effective) bulk modulus	$\mathrm{N/m^2}$
ϕ	Phase offset	rad
ρ	Density	$\mathrm{kg/m^3}$
ω	Angular speed	rad/s
A	Area	$\mathrm{m^2}$
A_{g}	Final groove area	$\mathrm{m^2}$
B	Friction coefficient	Nm/(rad/s)
B_{stator}	Magnetic flux density in the stator	T
C_{q}	Orifice flow coefficient	-
D	Displacement	$\mathrm{m^3/rad}$
f	Frequency	Hz
F	Force	N
h	Kinematic flow gradient	$\mathrm{m^3/s^2}$
I	Current	A
J	Rotational inertia	$\mathrm{kg\ m^2}$
k	1 for regular pump, 2 for tandem pump	-
k_{cl}	Classical eddy loss coefficient	$\mathrm{Ws/(kg\ T^{\alpha})}$
k_{exc}	Excess loss coefficient	$\mathrm{Ws^{1.5}/(kg\ T^{1.5})}$
k_{h}	Hysteresis loss coefficient	$\mathrm{Ws^2/(kg\ T^2)}$
L	Lever of piston force around drive axis	m
l_{g}	Groove length	m
m	Mass	kg
n	Exponent in groove area function	-
p	Pressure	$\mathrm{N/m^2}$
p_0	System pressure	$\mathrm{N/m^2}$
P	Power	W
r	Radius	m
R	Radius to relief groove	m
R_{el}	Resistance	Ω
R_{pp}	Piston pitch radius	m
T	Torque	Nm
v	Velocity	m/s
z	Number of pistons	-

References

[1] Lonnie J Love, Eric Lanke, and Pete Alles. *Estimating the Impact (Energy, Emissions and Economics) of the US Fluid Power Industry*. Number December. Oak Ridge National Laboratory, Oak Ridge, USA, 2012.

[2] Lauren A Lynch and Bradley T Zigler. Estimating Energy Consumption of Mobile Fluid Power in the United States. Technical Report November, National Renewable Energy Laboratory, 2017.

[3] Damiano Padovani, Pavlos Dimitriou, and Tatiana Minav. Challenges and solutions for designing Energy-Efficient and Low-Pollutant Machines in Off-Road hydraulics. *Energy Conversion and Management: X*, 21(December 2023):100526, 2024.

[4] Thomas Heeger. *Design of Electro-Hydraulic Energy Converters : With Focus on Integrated Designs and Valve Plate Rotation*, volume 1971 of *Linköping Studies in Science and Technology. Licentiate Thesis*. Linköping University Electronic Press, Linköping, June 2023.

[5] Liselott Ericson and Thomas Heeger. The Electrification of Material Moving Machines : An Overview of Opportunities and Challenges Regarding Noise. In *Proceedings of the Interdisciplinary Conference on Innovation, Design, Entrepreneurship, and Sustainable Systems (IDEAS), 24-27 November 2024, Recife, Brazil*. Springer, 2025. ISBN 9783031961724. Paper presented at conference, proceedings to be published.

[6] Thomas Heeger, Martin West, and Liselott Ericson. Harmonic Characterisation of Electrically Driven Pumps. In Liselott Ericson and Petter Krus, editors, *Advancements in Fluid Power Technology: Sustainability, Electrification, and Digitalization. Proceedings of the Global Fluid Power Society PhD Symposium 2024, 17-20 June, 2024, Hudiksvall, Sweden*. Springer, 2025. ISBN 9783031845048. Paper presented at conference, proceedings to be published.

[7] Jaroslav Ivantysyn and Monika Ivantysynova. *Hydrostatic pumps and motors: principles, design, performance, modelling, analysis, control, and testing*. Akademia Books International, New Delhi, 2001. ISBN 8185522162.

[8] Noah D. Manring. *Fluid Power Pumps and Motors: Analysis, Design and Control*. McGraw Hill Book CO, 2013. ISBN 0071812202.

[9] Thomas Heeger, Samuel Kärnell, and Liselott Ericson. Challenges for multi-quadrant hydraulic piston machines. *Energy Conversion and Management: X*, 22(March):100578, 2024.

[10] Liselott Ericson, Johan Ölvander, and Jan-Ove Palmberg. On Optimal Design of Hydrostatic Machines. In *Proceedings of the 6th International Fluid Power Conference (6. IFK), 1-2 April, 2008, Dresden, Germany*, pages 273–286, 2008.

[11] T.A. Minav, L.I.E. Laurila, and J.J. Pyrhönen. Axial Piston Pump Flow Ripple Compensation by Adjusting the Pump Speed with an Electric Drive. In *The Twelfth Scandinavian International Conference on Fluid Power, May 18-20, 2011, Tampere, Finland*, 2011.

[12] Colin O'Shea. Hydraulic flow ripple cancellation using the primary flow source. In *Proceedings of the BATH/ASME 2016 Symposium on Fluid Power and Motion Control (FPMC2016), September 7-9, 2016, Bath, UK*, pages FPMC2016–1783, 2016.

[13] Gudrun Mikota and Bernhard Manhartsgruber. a Novel Pulsation Compensator for Displacement Machines. In *14th International Fluid Power Conference, 19-21 March, 2024, Dresden, Germany*, pages 389–401, 2024.

[14] Jianing Liang, Jin-woo Ahn, and Dong-hee Lee. High Performance Hydraulic Pump System Using Switched Reluctance Drive. In *Proceeding of International Conference on Electrical Machines and Systems 2007, Oct. 8∼11, Seoul, Korea*, pages 1470–1475, 2007.

[15] Viral Mehta. *Torque Ripple Attenuation for an Axial Piston Swash Plate Type*. Phd thesis, University of Missouri - Columbia, 2006.

[16] Noah D. Manring, Viral S. Mehta, Frank J. Raab, and Kevin J. Graf. The Shaft Torque of a Tandem Axial-Piston Pump. *Journal of Dynamic Systems, Measurement and Control, Transactions of the ASME*, 129(3):367–371, 2007.

[17] Linköping University (Division of Fluid and Mechatronic Systems). Hopsan. https://liu.se/en/research/hopsan, accessed 2025-02-17.

[18] Liselott Ericson and Jonas Forssell. A Novel Axial Piston Pump/Motor Principle With Floating Pistons: Design and Testing. In *BATH/ASME 2018 Symposium on Fluid Power and Motion Control (FPMC2018), September 12-14, 2018, Bath, United Kingdom*, pages FPMC2018–8937. American Society of Mechanical Engineers, 2018.

[19] Peter A J Achten. Power Density of the Floating Cup Axial Piston Principle. In *Proceedings of the ASME 2004 International Mechanical Engineering Congress and Expo (IMECE2004), November 13-19, 2004, Anaheim, California, USA*, pages IMECE2004–59006. ASME, 2004.

[20] J O Palmberg. Modelling of Flow Ripple from Fluid Power Piston Pumps. In *Fluid power components systems: 2nd Bath International Fluid Power Workshop, Taunton, Somerset, United Kingdom*, pages 207–227, 1990.

[21] Jianzhen Qu, Juri Jatskevich, Chengning Zhang, and Shuo Zhang. Torque ripple reduction method for permanent magnet synchronous machine drives with novel harmonic current control. *IEEE Transactions on Energy Conversion*, 36(3):2502–2513, 2021.

[22] Andreas Johansson. *Design Principles for Noise Reduction in Hydraulic Piston Pumps*. Phd thesis, Linköping University, 2005.

[23] Eberhard Zwicker and Hugo Fastl. *Psychoacoustics: Facts and Models*. Springer-Verlag Berlin Heidelberg GmbH, second edition, 1999. ISBN 9783540650638.

[24] Zi-Qiang Zhu, Shaoshen Xue, Wenqiang Chu, Jianghua Feng, Shuying Guo, Zhichu Chen, and Jun Peng. Evaluation of Iron Loss Models in Electrical Machines. *IEEE Transactions on Industry Applications*, 55(2):1461–1472, 2019.

[25] Muhammad Sohail Ahmed. *Effect of harmonics on iron losses*. Master thesis, Chalmers University of Technology, 2007.